Physica B 405 (2010) 4267–4270

Contents lists available at ScienceDirect

Physica B

journal homepage: www.elsevier.com/locate/physb

Self-consistent calculation of transport properties in Si δ−doped GaAs quantum wells as a function of the temperature

L.M. Gaggero-Sager [a], G.G. Naumis [a,c,*], M.A. Muñoz-Hernandez [b], V. Montiel-Palma [b]

[a] Facultad de Ciencias, Universidad Autónoma del Estado de Morelos, Av. Universidad 1001, Col. Chamilpa, 62209 Cuernavaca, MOR., Mexico
[b] Centro de Investigaciones Químicas, Universidad Autónoma del Estado de Morelos, Av. Universidad 1001, Col. Chamilpa, 62209 Cuernavaca, MOR., Mexico
[c] Departamento de Física-Química, Instituto de Física, UNAM. Apdo. Postal 20-364, 01000, México D.F., Mexico

ARTICLE INFO

Article history:
Received 1 May 2010
Received in revised form
22 June 2010
Accepted 10 July 2010

Keywords:
Delta doping
Semiconductors
Quantum wells

ABSTRACT

The electronic structure of a delta-doped quantum well of Si in GaAs is studied at different temperatures. The calculation is carried out self-consistently in the framework of the Hartree approximation. The energy levels and the mobility trends are reported for various impurity densities. As a consequence, the temperature dependence of the mobility can be explained by means of the temperature variation of the electronic structure. The calculated ratios between mobilities at 300 and 77 K, at different impurity densities, are in excellent agreement with the experimental data. These results can also be extrapolated to other similar systems like B, GaN, InSb, InAs and GaAs.

1. Introduction

Nowadays, semiconductor doping down to atomic resolution (δ doping) is possible due to the spectacular precision of molecular beam epitaxy growth. Such doping technique has many new potential applications in electronic devices [1] including field effect transistors. Most of the work on δ−doped systems has been made primarily on n-type structures [2–5]. At the same time, there are several experimental works in which an enhancement in the transport properties of double and triple delta-doped quantum wells in different materials is reported [6–10]. However, there are some apparently contradictory reports in Si delta-doped GaAs wells [6,7]. For example, Zheng et al. [6] measured the mobility of single and double delta-doped wells as a function of the temperature. They found an increase in the mobility by a factor of 2.5 from 77 to 300 K. Such result was very surprising since for this kind of system, a broad mobility peak near the liquid nitrogen temperature was expected [11–13]. Motivated by this unexpected result, Gurtovoi and coworkers [7] accomplished transport measurements in single and double delta-doped systems, but they never found the trend observed by Zheng et al. [6]. Since the only difference between the two sets of experiments was the doping level, one can formulate the hypothesis that doping is able to modify the shape of the electronic structure. However, the explanation for such disagreement is still an open question, mainly because from a theoretical point of view, there are few reports dealing with temperature effects and transport properties in delta-doped systems [14–18]. None of these reports is aimed to explain the apparent contradiction between sets of experimental results [6,7]. In the present paper, we will show that the changes in the electronic structure are responsible for these apparent contradictions between different sets of experiments. It becomes evident that modeling such changes is not trivial since the electronic structure must fulfill at the same time the Schrödinger equation, the set of Maxwell equations, the Fermi–Dirac statistics and comply with electric neutrality [21,22,24–28]. Herein we present such a full self-consistent calculation. The layout of this work is the following, in Section 2 we develop the model and the corresponding equations. In Section 3, the results are presented. Finally, the conclusions are given in Section 4.

2. Model

Consider an electron in a δ doped semiconductor in which the z axis is chosen perpendicular to the δ impurity layer. The corresponding Schrödinger equation for the z direction in the framework of the Envelope Function Approximation (EFA) is

$$-\frac{\hbar^2}{2m^*}\frac{d^2}{dz^2}F_i(z)+V(z)F_i(z)=E_iF_i(z). \quad (1)$$

Here $F_i(z)$ is the z-dependent envelope wave function of the electron, E_i the i-th energy level, m^* the effective mass in the

* Corresponding author. Tel.: +555 5622 51 74; fax: +555 5622 50 08.
E-mail address: naumis@fisica.unam.mx (G.G. Naumis).

0921-4526/$ - see front matter © 2010 Elsevier B.V. All rights reserved.
doi:10.1016/j.physb.2010.07.022

semiconductor and $V(z)$ the potential due to the δ doping and the polarization of the medium.

The spatial band bending of the previous equation is described by the Poisson equation. To improve accuracy and convergence, the energy origin is taken at $z=0$ ($V(0)=0$), and the electric field tends to zero when $z\to\infty$. Integrating twice and using the Fubini–Lebesgue theorem to change the order of integration, the Poisson equation adopts a simple form which provides the potential:

$$V(z)=\frac{4\pi e}{\epsilon_r}\int_0^z(z-\chi)\rho_e(\chi)\,d\chi+\frac{2\pi e^2}{\epsilon_r}n_{2D}|z|, \tag{2}$$

where n_{2D} is the bidimensional impurity concentration at the impurity layer ($\rho_{imp}=n_{2D}\delta(z)$), ρ_e is the free charge density in the well region and ϵ_r is the dielectric constant. The next ingredient is that the solution must fulfill the Fermi–Dirac statistics. Such condition allows to obtain the charge density, $\rho_e(z)$, which is given by

$$\rho_e(z)=-\frac{em^*k_BT}{\pi\hbar^2}\sum_{i=1}^{n}\ln\left[1+\exp\left(\frac{E_F-E_i}{k_BT}\right)\right]|F_i(z)|^2, \tag{3}$$

where E_F is the Fermi level and n is the occupation number. For nonvanishing temperatures, all levels are in principle occupied. Nevertheless, if the system is locally neutral, the continuous part of the spectrum may be considered empty. Then, the sum in Eq. (3) is extended only up to the value of the occupation number in the band. At the same time, the charge neutrality requires that $en_{2D}=-\int_{-\infty}^{\infty}\rho_e(\chi)\,d\chi$. As a result, the Fermi level is given implicitly by

$$en_{2D}=\frac{em^*k_BT}{\pi\hbar^2}\sum_{i=1}^{n}\ln\left[1+\exp\left(\frac{E_F-E_i}{k_BT}\right)\right]. \tag{4}$$

The calculations to obtain the energy levels and wave functions consist on the simultaneous solution of the Schrödinger and Poisson equations [23], given by Eqs. (1) and (2), using the restrictions imposed by Eqs. (3) and (4). The solutions are rather awkward and sometimes present divergences. In the present work, iterations were performed using at each step an input potential given by Eq. (2) to solve Eq. (1). Then, an output potential is calculated using Eqs. (3) and (4) in Eq. (2). Throughout this process, a careful mixing of the input and output potentials from the step of the previous iteration is fundamental, since it allows for the quickest convergence and hence non-divergence.

Let us explain briefly how this mix is done. First a bidimensional space is generated by graphing the input potential at point z in the X-axis, and the output potential at the same point z on the Y-axis. Since the self-consistent solution is achieved when the input and output potentials are identical, this solution would be the set of points in the line with slope 1, corresponding to $X=Y$. If $V^{m\ in}(z)$ ($V^{m\ out}(z)$) is the input (output) potential in the step m of self-consistency, in general the corresponding point in this space will not be in the line $X=Y$. However, we can construct a straight line by using two points from the previous steps of self-consistency. By finding the intersection between this line and the $X=Y$ line, we can obtain the next input potential. Since the zero of energies was placed at the origin, the mixture can be made in the following manner,

$$V^{(m+1)i}(z)=A(z)V^{m\ in}(z)+(1-A(z))V^{m\ out}(z) \tag{5}$$

where

$$A(z)=\begin{cases}\dfrac{V^{m\ out}(z)-V^{(m-1)\ out}(z)}{V^{m\ out}(z)-V^{(m-1)\ out}(z)-V^{m\ in}(z)+V^{(m-1)\ in}(z)} & \text{if } \Delta V^m(z)\,\Delta V^{(m-1)}(z)\le 0\\ \dfrac{|V^{m\ in}(z)|}{V^{m\ in}_{\max}(\infty)}\beta & \text{in other case}\end{cases} \tag{6}$$

$V^{m\ in}_{\max}(\infty)$ is the absolute value of the maximum value of the input potential in step m, $\beta=1-m/n_{\max}$ and $n_{\max}$ is the maximum number of iterations proposed to be carried out. $n_{\max}$ changes, but it is usually around $n_{\max}\sim 200$ and $\Delta V^m(z)=V^{m\ in}(z)-V^{m\ out}(z)(\Delta V^{(m-1)}(z)=V^{(m-1)\ in}(z)-V^{(m-1)out}(z))$. The first part of the equation for $A(z)$ demands both points (corresponding to steps m and $m-1$) to be on both sides of the line $X=Y$ to avoid divergence. The second part of the equation for $A(z)$, at the origin, $V^{(m+1)\ i}(0)=V^{m\ out}(0)$, so that the input potential of step $m+1$ slowly begins to differentiate itself from the output potential from step m as it distances itself from the origin.

Using the described self-consistent procedure, we calculated the resulting self-consistent potential, energy levels and wave functions. Once the calculations were finished, we obtained the relative mobility due to ionized impurities between $T=77$ and 300 K, using a formula derived in Ref. [18]

$$\mu_{rel}=\frac{\mu^{T=300\,\mathrm{K}}}{\mu^{T=77\,\mathrm{K}}}=\frac{k_BT^{Ni}\sum_{i=1}^{n_{Ni}}\ln\left[1+\exp\left(\dfrac{E_F^{Ni}-E_i^{Ni}}{k_BT}\right)\right]\int|F_i^{Ni}(z)|^2|z|\,dz}{k_BT^{R}\sum_{i=1}^{n_R}\ln\left[1+\exp\left(\dfrac{E_F^{R}-E_i^{R}}{k_BT}\right)\right]\int|F_i^{R}(z)|^2|z|\,dz} \tag{7}$$

where the superscripts Ni and R are used to denote quantities evaluated at 77 and 300 K, respectively. Notice that here we only calculate the relative mobility between temperatures, which is the main objective of the paper. The calculation of the actual value of the mobility at a given temperature is much more difficult. Also, it is known from the work of Ando, Fowler and Stern [29], that the inter-band scattering is very important for transport in two dimensional systems, specially when two or more sub-bands are occupied, as for example in $Si-SiO_2$ interfaces. Thus, in principle we need to consider not only the interaction with the ionized delta impurity layer, but also a contribution from the inter-band scattering. A similar approach to the one used for the impurity contribution can be used to include such effect. To do this, let us consider the charge density of the sub-band i. This density is given by Eq. (3)

$$N_i(z)=-\frac{em^*k_BT}{\pi\hbar^2}\sum_{i=1}^{n}\ln\left[1+\exp\left(\frac{E_F-E_i}{k_BT}\right)\right]|F_i(z)|^2, \tag{8}$$

which can be written as

$$N_i(z)=n_i|F_i(z)|^2,$$

where n_i is the occupation number of the sub-band i. Now we can calculate the relative mobility due to the sub-band interaction as in Eq. (7)

$$\mu_{rel}^{inter}=\frac{\mu_{inter}^{T=300\,\mathrm{K}}}{\mu_{inter}^{T=77\,\mathrm{K}}}=\frac{k_BT^{Ni}\sum_{i=1}^{n_{Ni}}\sum_{j=i+1}^{n_{Ni}}\int\int N_i^{Ni}(z)N_j^{Ni}(z')|z-z'|\,dz\,dz'}{k_BT^{R}\sum_{i=1}^{n_R}\sum_{j=i+1}^{n_{Ni}}\int\int N_i^{R}(z)N_j^{R}(z')|z-z'|\,dz\,dz'}. \tag{9}$$

3. Results and discussion

The following values were used as input parameters $m^*=0.067m_0$; m_0 being the free electron mass, $\epsilon_r=12.5$, and $n_{2D}=3\times10^{12}$ and $5\times10^{12}\,\mathrm{cm}^{-2}$. A variation of less than 0.01 meV in the depth of the well for two consecutive steps was taken as the convergence criterion.

In Figs. 1 and 2, we show the results of this procedure at two different doping concentrations. In each figure, the resulting self-consistent potential $V(z)$ and the envelope probability $|F_i(z)|$ centered at its energy level are shown at 77 and 300 K. The first important observation is that the depth of the potential is increased at high temperatures, and some new energy levels

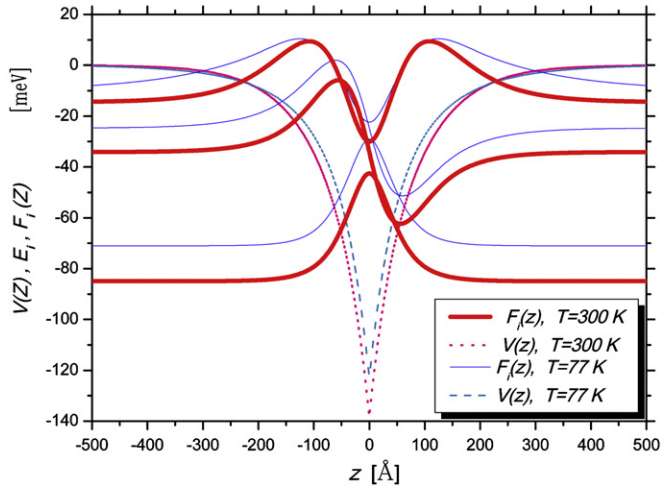

Fig. 1. Potential profile, energy levels and square wave functions of Si δ−doped GaAs quantum wells for an impurity density of $3\times10^{13}\,cm^{-2}$. The thin solid lines (blue on line) correspond to wave functions at 77 K, and the thick solid lines (red on line) at 300 K. The dashed (dotted) line denotes the potential $V(z)$ at 77 K (300 K). (For interpretation of the references to colour in this figure legend, the reader is referred to the web version of this article.)

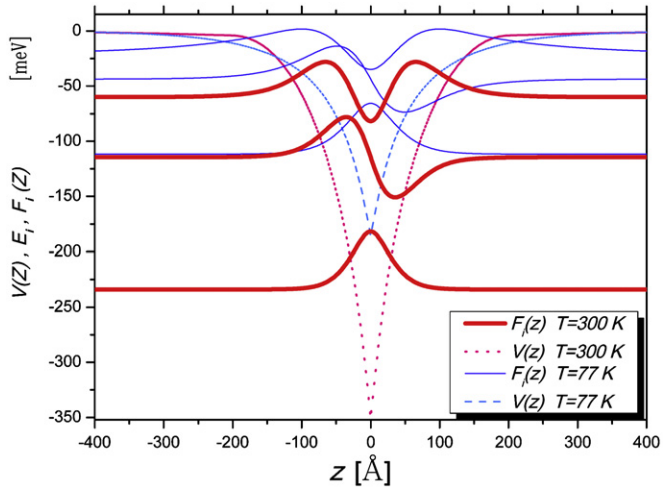

Fig. 2. Potential profile, energy levels and square wave functions of Si δ−doped GaAs quantum wells for an impurity density of $5\times10^{13}\,cm^{-2}$. The thin solid lines (blue on line) correspond to wave functions at 77 K, and the thick solid lines at 300 K (red on line). The dashed (dotted) line denote the potential $V(z)$ at 77 K (300 K). (For interpretation of the references to colour in this figure legend, the reader is referred to the web version of this article.)

appear. In the case of $n_{2D}=3\times10^{12}\,cm^{-2}$, one level appears, while for $n_{2D}=5\times10^{12}\,cm^{-2}$ three new levels appear. This is a clear indication that doping and temperature have a strong influence on the electronic structure. The appearance of new levels as the temperature is raised can be understood as a consequence of the increased depth of the self-consistent potential, which at the same time is a result of the delicate interplay between the electrical neutrality condition and the tendency for an increased average kinetic energy.

Before comparing our theoretical calculations with the experimental results, certain considerations are needed. For example, Gurtovoi et al. [7] have shown that if the mobility of a group of electrons in higher sub-bands is increased, the measured concentration decreases and it can be lower than the net sub-band concentration. Thus, the product of the sheet concentration and mobility is a more realistic criterion to evaluate the sample quality. On the other hand, the double well system at a certain interwell distance behaves like a single well one, so in the specific case of Ref. [7], this criteria is reached at 350 Å. However, in single quantum wells with $n_{2D}=3\times10^{12}\,cm^{-2}$, the measured concentration [7] is very different for 77 and 300 K. In the double delta-doped quantum well, a small variation of the concentration is also observed for interwell distances of 380 and 580 Å. In principle, the carrier concentration should remain unchanged with a variation of the interwell distance since the impurity density is always the same. The observed variations in Ref. [7] can also be due to the experimental error, so here we will compare our results for the mentioned interwell distances, 380 and 580 Å, since they seem to be the most consistent data sets. For both distances, the mobility decreases with temperature, with relative values of 0.81 and 0.88, respectively. Taking into account that the electronic structure is the same in both cases, we can average the results for 380 and 580 Å and consider that the relative mobility for a single delta-doped well with an impurity concentration of $3\times10^{12}\,cm^{-2}$ is 0.85. The relative mobility due only to the delta impurity gives 0.88 in our theoretical calculation.

Zheng et al. [6] have grown a variety of double and single delta-doped quantum wells. The impurity concentration in all of their samples was $n_{2D}=5\times10^{12}\,cm^{-2}$. Despite of all the data reported by these authors, here we are only interested on the results presented for the single delta-doped wells. In this system, the Hall mobility was measured and an increase factor of 2.5 was observed when the temperature is increased from 77 to 300 K. In the case of a double delta-doped well with an interwell distance of 400 Å, the Hall mobility is enhanced by a factor of 1.7. So, using the same average procedure as in the data reported by Gurtovoi et al. [7], and with the purpose of taking into account the experimental error, we see an increase in the Hall mobility by a factor 2.1 ± 0.4. In our theoretical computations considering only the impurity contribution, this factor is 1.97. The agreement of our theoretical results with the experimental data, seems to point that the main contribution to the mobility comes in this case from the interaction with the delta-doped layer. However, we can use Eq. (9) to evaluate how the inter sub-band scattering scales with temperature. We start by observing that from the calculated potential and the corresponding wave functions, the integrals that appear in Eq. (9)

$$\int\int |F_i(z)|^2|F_j(z)|^2|z-z'|\,dz\,dz', \tag{10}$$

do not change much with temperature, as is also clear from a visual inspection of the figures. Thus, from Eq. (9) we can write

$$\mu_{rel}^{inter}\approx\frac{\sum_{i=1}^{n_{Ni}}\sum_{j=i+1}^{n_{Ni}}n_i^{Ni}n_j^{Ni}}{\sum_{i=1}^{n_R}\sum_{j=i+1}^{n_{Ni}}n_i^{R}n_j^{R}}. \tag{11}$$

By using the calculated values for n_i^{Ni} and n_i^{Ni}, we obtain that in the case of $n_{2D}=5\times10^{12}\,cm^{-2}$, μ_{rel}^{inter} has the value 2.4. Such value is slightly bigger than the experimental value, and also bigger than the theoretical result considering only the impurity for $n_{2D}=5\times10^{12}\,cm^{-2}$. A similar calculation for $n_{2D}=3\times10^{12}\,cm^{-2}$ gives 0.86, which scales almost as the impurity mobility. From these results, we can observe that the impurity and inter sub-band contributions scale with temperature in a very similar way. From our calculation it is not possible to decide which contribution dominates, since here we only have relative mobilities, although a comparison with the experimental data shows evidence of a dominant impurity contribution. In any case, the similar scaling of the impurity and inter sub-band scattering can be understood basically as a consequence of the global changes in the electronic structure with the temperature.

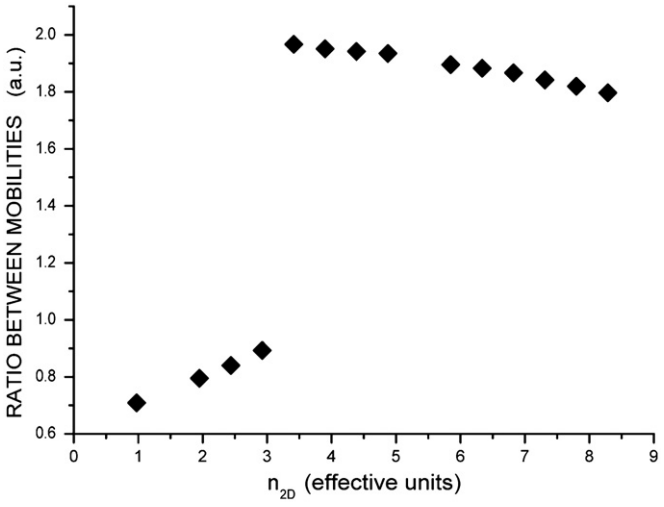

Fig. 3. Ratio between mobilities (77 K/300 K) at different impurity concentrations.

4. Conclusions

In conclusion, the Hall mobility in single delta-doped wells presents an enhancement with temperature by a factor of 0.85 for impurity concentrations of $n_{2D}=3\times10^{12}\,\mathrm{cm}^{-2}$, and 2.1 for $n_{2D}=5\times10^{12}\,\mathrm{cm}^{-2}$, while our results give the values of 0.88 and 1.97, respectively, considering only the impurity contribution to the mobility. If the inter sub-band scattering is considered, the ratios of such contributions are 0.86 and 2.4, respectively. All of the previous results show that the delta-doped wells present a completely different behavior depending on the impurity concentrations. Thus, the study of these systems cannot be generalized readily. Indeed, the report of Gurtovoi et al. [7] assumes that the data presented by Zheng and colleagues [6] can be faulty, however, as we already demonstrated here, both apparent discrepancies are explained by changes in the electronic structure.

The relative mobility at different concentrations of impurities is presented in Fig. 3. Comparison of the relative mobility changes allows for the following observations. At n_{2D} values higher than $3\times10^{12}\,\mathrm{cm}^{-2}$, the relative mobility increases with the temperature. In contrast, for $n_{2D}\leq3\times10^{12}\,\mathrm{cm}^{-2}$ the relative mobility increases with the concentrations while it decreases for $n_{2D}>3\times10^{12}\,\mathrm{cm}^{-2}$. Theses findings show that there is a change in the conductivity behavior with respect to the temperature and the impurity concentration for $n_{2D}>3\times10^{12}\,\mathrm{cm}^{-2}$.

Applying dimensional analysis, these results could also be extrapolated to other systems with very similar band structures. We should expect for instance, for n type delta-doped quantum wells, a critical point around $n_{2D}=3.5\times10^{13}\,\mathrm{cm}^{-2}$ in GaN, $n_{2D}=8\times10^{10}\,\mathrm{cm}^{-2}$ in InSb and $n_{2D}=3\times10^{11}\,\mathrm{cm}^{-2}$ in InAs. Experiments are need to be carried out in order to verify these predictions.

Si delta-doped GaAs QW's have a quite different behavior with respect to B delta-doped Si QW's [16], contrary to what should be supposed. In the case of B delta-doped Si wells, the electronic structure changes dramatically with temperature. For example, the number of levels goes from 7 at 0 K to 13 at room temperature while in the system reported here the trend is opposite, i.e., the number of levels remains practically unchanged as seen in Figs. 1 and 2. The Fermi level (measured from the band bottom) goes down about 70 meV from 0 to 300 K for B delta-doped Si wells, while in Si delta-doped GaAs wells this dropping is only about half, 30 meV.

There is also experimental evidence in p-type delta-doped quantum wells in GaAs that supports our findings. Noh et al. observed that the resistivity behaves quite different for different impurity densities [19,20]. Of course, we do not aim to explain the aforementioned experimental data, but such experimental results point in the same direction.

In summary, Si-delta-doped GaAs systems present a notably different behavior with temperature as compared to B-delta-doped quantum wells in Si. Despite the similarities in both systems (both due to planar doping), it is not possible to extrapolate the trends from one system to another. All seems to indicate that each quantum well will attend a particular behavior with temperature.

We would like to thank DGAPA project IN100310-3 for financial support.

References

[1] J.-h. Zhu, D.-w. Gong, B. Zhang, F. Lu, C. Sheng, H.-h. Sun, X. Wang, Phys. Rev. B. 52 (1995) 8959.
[2] R.L. Headrick, B.E. Weir, A.F.J. Levi, D.J. Eaglesham, L.C. Feldman, Appl. Phys. Lett. 57 (1990) 2779.
[3] W.-X. Ni, G.V. Hansson, J.-E. Sundgren, L. Hultman, L.R. Wallenberg, J.-Y. Yao, L.C. Markert, J.E. Greene, Phys. Rev. B 46 (1992) 7551.
[4] H.-J. Gossmann, C.S. Rafferty, A.M. Vredenberg, H.S. Luftman, F.C. Unterwald, D.J. Eaglesham, D.C. Jacobson, T. Boone, J.M. Poate, Appl. Phys. Lett. 64 (1994) 312.
[5] Y. Wang, R.J. Hamers, E. Kaxiras, Phys. Rev. Lett. 74 (1995) 403.
[6] X. Zheng, T.K. Carns, K.L. Wang, B. Wu, Appl. Phys. Lett. 62 (1993) 504.
[7] V.L. Gurtovoi, V.V. Valyaev, S.Y. Shapoval, A.N. Pustovit, Appl. Phys. Lett. 72 (1998) 1202.
[8] C.L. Wu, W.C. Hsu, H.M. Shieh, W.C. Liu, Appl. Phys. Lett. 64 (1994) 307.
[9] M.J. Kao, W.C. Hsu, R.T. Hsu, Y.H. Wu, T.Y. Lin, C.Y. Chang, Appl. Phys. Lett. 66 (1995) 2505.
[10] H.H. Radamson, M.R. Sardela Jr., O. Nur, M. Willander, B.E. Sernelius, W.-X. Ni, G.V. Hansson, Appl. Phys. Lett. 64 (1994) 1842.
[11] E.F. Schubert, J.E. Cunningham, W.T. Tsang, Solid State Comm. 63 (1987) 591.
[12] N. Pan, J. Carter, G.S. Jackson, H. Hendriks, X.L. Zheng, H.M. Kim, Appl. Phys. Lett. 59 (1991) 458.
[13] P.M. Koenraad, F.A.P. Blom, C.J.G.M. Langerak, M.R. Leys, J.A.A.J. Perenboom, J. Singleton, S.J.R.M. Spermon, W.C. van der Vleuten, A.P.J. Voncken, J.H. Wolter, Semicond. Sci. Technol. 5 (1990) 861.
[14] P.M. Koenraad, A.C.L. Heessels, F.A.P. Blom, J.A.A.J. Perenboom, J.H. Wolter, Physica B 184 (1993) 221.
[15] G.-Q. Hai, N. Studart, F.M. Peeters, Phys. Rev. B 52 (1995) 11273.
[16] L.M. Gaggero-Sager, R. Pérez-Alvarez, Appl. Phys. Lett. 70 (1997) 212.
[17] E. Ozturk, Y. Ergun, H. Sari, I. Sokmen, Eur. Phys. J. AP 21 (2003) 97.
[18] I. Rodriguez-Vargas, L.M. Gaggero-Sager, J. Appl. Phys. 99 (2003) 033702.
[19] J.P. Noh, F. Shimogishi, N. Otsuka, Phys. Rev. B 67 (2003) 075309.
[20] J.P. Noh, F. Shimogishi, Y. Idutsu, N. Otsuka, Phys. Rev. B 69 (2004) 045321.
[21] G.A.M. Hurkx, W. Van Haeringen, J. Phys. C: Solid State Phys. 18 (1985) 5617.
[22] C.D. Simserides, G.P. Triberis, J. Phys.: Condens. Matter 5 (1993) 6437.
[23] H. Akai, P.H. Dederichs, J. Phys. C: Solid State Phys. 18 (1985) 2455.
[24] W. Xu, J. Mahanty, J. Phys.: Condens. Matter 6 (1994) 4745.
[25] C.D. Simserides, G.P. Triberis, J. Phys. C: Solid State Phys. 8 (1996) 2455.
[26] W. Xu, Europhys. Lett. 40 (1997) 411.
[27] T.J. Green, W. Xu, J. Appl. Phys. 88 (2000) 3166.
[28] W. Xu, P.A. Folkes, G. Gumbs, J. Appl. Phys. 102 (2007) 033703.
[29] T. Ando, A.B. Fowler, F. Stern, Rev. Mod. Phys. 54 (1982) 437.